J. Materials, Conc. Struct., Pavements, JSCE, No. 592／V-39, 155-167, 1998 May

EXPERIMENTAL STUDY ON INTERFACIAL TRANSITION ZONES IN REINFORCED CONCRETE

Nobuaki OTSUKI[1], Makoto HISADA[2], Nathaniel B. DIOLA[3] and Tarek UDDIN Md.[4]

[1]JSCE Member, Dr. of Eng., Professor, Dept. of Int'l. Development Eng., Tokyo Institute of Technology
(2-12-1 O-okayama, Meguro-ku, Tokyo 152-8552, Japan)
[2]JSCE Member, Dr. of Eng., Associate Professor, Dept. of Civil Eng. and Architechture, Niigata University
(8050 Ikarashi 2, Niigata-shi, Niigata 950-2185, Japan)
[3]Graduate Student, Department of Civil Engineering, Tokyo Institute of Technology
(2-12-1 O-okayama, Meguro-ku, Tokyo 152-8552, Japan)
[4]Civil Engineer, Dr. of Eng., Overseas Civil Eng. Dept., Int'l. Operations, Osaka Head Office, NEWJEC Inc.
(20-19 Shimanouchi 1-chome, Chuo-ku, Osaka 542-0082, Japan)

The study compared the aggregate-matrix and steel bar-matrix interfacial transition zones (ITZs) with the purpose of determining their characteristics, differences, and factors affecting them.

Factors in consideration include type of mineral admixtures, mix proportion, steel bar orientation with respect to casting direction, and others.

Results include description of the ITZs and its properties. It was also found out that there is a great difference between the two ITZs specifically with respect to the use of admixtures and gap formation under the aggregates or horizontal steel bars.

Key Words: *interfacial transition zone (ITZ), gaps, transition region, aggregates, reinforcing bars, corrosion*

1. INTRODUCTION

In recent history of concrete use where new problems such as those of durability are increasing, the need to understand concrete deeper has become urgent. Concrete, as viewed from the material science point of view has become a lively subject of discussion. Together with the advancements in the field of material science, the study of concrete's individual components and their interactions has captured the attention of many researchers.

Studies on the interaction between aggregates and cement pastes in France(1948) revealed for the first time the existence of a region between the aggregate and the bulk paste with characteristics different from either material. It was then called "transition aureole"[1)] which in recent literature, evolved into "interfacial transition zone" (hereafter referred to as ITZ). However, an exact definition of an ITZ is hard to find in the literature.

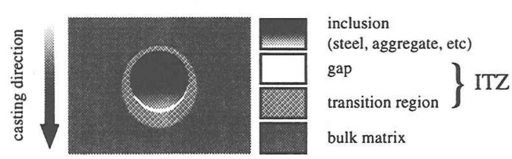

Fig. 1 Schematic Representation of the ITZ

With reference to **Fig. 1**, an ITZ is defined in this paper as:

*a region adjacent to any inclusion in concrete. It is composed of a **gap,** which may not be present at all times, and a **transition region,** which is a matrix affected by the presence of the inclusion.*

Until now, studies on the ITZs have been conducted mainly on aggregate-paste systems. In the case of steel-paste ITZs, investigations have been carried out using steel fibers/wires and also flat, polished steel surfaces. However, studies using reinforcing steel bars are scarce.

In the present investigation, two ITZs were considered namely that of aggregate and matrix and that of reinforcing steel bar and matrix.

Matrix is a collective term used to refer to paste, mortar, and concrete.

2. LITERATURE SURVEY

(1) Introduction

Various investigations dealing with the ITZs under consideration are reviewed. It should be noted that previous studies on the ITZs did not consider the existence of the gaps. Hence, the term *"ITZ"* in these studies corresponds to *"transition region"* as previously defined.

(2) The Aggregate-Paste ITZ

a) Formation Mechanism

Recent publications directly or indirectly support the "through solution" mechanism[2] of cement hydration which is exemplified by Maso's hypothesis[3),4)]. The hypothesis explained the formation of hydration products but not the cause of the initial high water content or high porosity near the surface. To account for this, three mechanisms namely "wall effect"[5)], arch-shaped grain arrangement in contact with the rock[4)], and effect of vibration[6)] were proposed but these still need verification by other researchers.

b) Morphology

Plain OPC Pastes

In general, the microstructure at the aggregate-paste transition region can be divided into two parts: a ~1 μm layer in contact with the aggregate and a paste region which may extend to some 50μm or more which is affected by the presence of the aggregate[5)]. Some researchers[7),8)] showed that the thin layer is composed of CH and C-S-H and thus termed as "duplex film". Others[9),10)] however detected only C-S-H. It was suggested that the reason for this lies in the aggregate properties, specifically its size[5)]. It is important to note here that not all researchers were able to detect the "duplex film"[9),11)].

The paste region affected by the presence of aggregate can be characterized as follows: 1) increasing porosity, CH, and C-S-H gradients and decreasing anhydrous cement content as the aggregate is approached[12)], 2) inherent weakness of this zone which causes microcracks to form here under any external stress[11)] and 3) formation of preferential fracture planes due to non-random orientation of the CH crystals which cleaves easily along its basal plane[9)].

Pastes with Mineral Admixture

In a recent review, Bentur and Odler[13)] summarized the effects of silica fume on the transition regions. The change as compared to systems without silica fume include reduction of transition zone thickness, significant reduction in the amount of CH especially after long hydration times and reduction of preferential orientation of CH. These effects were attributed to both physical and chemical properties of silica fume. Due to its size, efficient packing near the interface can be achieved, and chemically, silica fume is highly pozzolanic and reacts to form C-S-H, at the expense of $Ca(OH)_2$.

Type F fly ash (5% cement replacement), when mixed with Portland cement, showed no significant changes in the transition region structure[14)]. In a study by Carles-Guibergues, et. al.[quoted in 15)] however, fly ash with porous grains reduced the zone size substantially while the use of fly ash from calcareous lignite or iron slag showed tendency to increase the zone size.

Thickness of the Aggregate-Paste Transition Region

The ITZ, being a separate phase should have (at least hypothetically) a volume or some dimension such as thickness. Determination of this 'thickness' has been an issue and values reported were dependent on the method of measurement and the definition of 'thickness' itself. For example, arguing from the view of particle packing and cement grain size, Scrivener[5)] estimated the effective transition region thickness to be at least 50μm within which, a narrower 20μm from the aggregate has a more pronounced difference in properties as compared to the bulk paste. In another case, Snyder, et. al.[from 5)] reported a value of 15~20μm which is the range that best explains their MIP (Mercury Intrusion Porosimetry) data.

c) Transition Region Microhardness

Several authors have used microhardness measurement in the study of the ITZs. Mindess[16)] stated the different problems encountered in microhardness testing which include the use of very small loads in order to create small indentations, and the dependence of test results on the smoothness of the surface. Thus, hardness values obtained by some authors vary[from 16)]: Mehta and Monteiro(1988) obtained ~1 kg/mm^2, Lyubimova and Pinus(1962) got 10-15 kg/mm^2 while Wang (1988) reported 10-30 kg/mm^2.

d) The Aggregate-Paste ITZ as it Relates to Durability of Concrete Structures

It has been recognized that due to the inherent high porosity in the ITZ, the ITZ plays an important role in the durability of concrete, specifically, in its transfer properties. Recent reviews have been made regarding its effect on concrete's transfer properties[17)] and on the action of environmental conditions[18]. Suffice it to say that even though direct experimental evidence of the influence of environment on the ITZs is limited, the factors affect the ITZ in the same way as the bulk concrete. Improvements in the bulk concrete such as mechanical strength is also accompanied by reduction in porosity and permeability but a generalization of the procedures still faces technical as well as financial difficulties[18].

(3) The Steel-Paste Interfacial Transition Zone

Investigations on the steel-paste ITZ can be divided into 3 groups depending on the form of the steel used: 1) *steel bar*, 2) *steel fiber/wire*, and 3) *steel plate*. 1) and 3) can be classified as *fixed* wherein movement of the steel during casting is restricted as opposed to 2) in which the fiber/wire can move (*free*). This may lead to differences in the ITZ structure.

Most of the studies regarding this ITZ has focused on the second group while only very few used steel bars (group 1). The third group is mainly characterized by casting paste/mortar against a flat steel surface. In the following review, care will be taken to differentiate between the three.

a) Formation Mechanism

The formation mechanism of the transition region around steel fibers is taken to be similar to that of the aggregate[13]. The porous nature of the transition region is attributed to inefficient packing of cement particles due to "wall effect"[4),5]. For the case of steel wires, the effect of vibration had been identified as one reason for the inefficient packing and resulting higher local W/C, and thus increased porosity near the interface[6].

b) Morphology

Plain OPC Pastes

Studies on the ITZ between reinforcing steel bars and pastes have been scarce. With regard to morphology, Mindess[19] stated that it is similar to that of steel fiber-paste transition region. In a recent review, Bentur, et.al[14] pointed out that the steel fiber-paste transition zone morphology is quite similar to that observed around aggregates in concrete. In effect, the reinforcing steel-paste transition region is similar to that of aggregate-paste.

In general, the microstructure of the steel fiber-paste transition region can be characterized as being more porous than the bulk paste and rich in CH, which is mostly in contact with the fiber surface.

These observations points out that the aggregate-paste and steel-paste ITZs are similar but it will be shown later in this paper that there is a difference between them specially when the interfacial gaps are considered.

Effect of Mineral Admixtures

The richness in CH was still observed even with addition of admixtures. SEM observations revealed solid films of large CH crystals over most of the steel surface even in the presence of condensed silica fume (16% by weight)[20].

Thickness

As mentioned previously, the values of 'thickness' of the transition region that can be found in the literature were dependent on the definition of thickness and measurement method. For the steel-paste case, an estimate of the thickness was provided by Wei, et.al.[21] who reported the value to be 80μm: the point beyond which the microhardness of the paste around a steel-fiber became constant.

c) Transition Region Microhardness

Microhardness tests done by Wei, et. al.[21], found that the microhardness values were lowest around 25 to 35 μm from the surface of a 0.5mm fiber and microhardness values increased with decrease in water to cement ratio.

d) Microstructure and Corrosion of Reinforcement

The kind of microstructure formed around the steel is of great importance in corrosion protection. Page[22] pointed out that the presence of CH in direct contact with the steel will modify the electrode characteristics of the metal. Since the CH film covers a considerable fraction of the metal surface, oxygen is screened and this also provides an alkaline buffer, which is necessary for passivation.

Monteiro, et. al's.[20] study on the effects of silica fume addition revealed that corrosion occurred only in the silica fume-containing systems and attributed this to the probable higher Cl^-/OH^- ratio in the pore solution. (They used composite specimens made by casting paste against a polished cross section of a 1.9mm steel bar.) This is consistent with a previous study claiming that increasing additions of silica fume reduced both the alkalinity and the chloride binding ability of the paste[23].

3. OBJECTIVES

The ITZs were studied with the following two objectives: 1) To clarify the difference between the aggregate-matrix and steel-matrix ITZs if such difference exists and 2) To identify and describe the general features of the ITZs.

Table 1 Physical and Chemical Properties of Ordinary Portland Cement (OPC) and Mineral Admixtures

	OPC	FA	BFS	SF
Specific Gravity	3.14	2.18	2.89	2.24
Blaine Fineness, cm^2/g	3270	3240	8010	205500
Loss on Ig., %	0.60	1.74	1.20	1.38
SiO_2 %	21.30	50.71	32.30	97.50
Al_2O_3 %	5.30	24.12	13.80	0.41
CaO %	64.40	10.01	41.50	0.19
MgO %	2.20	2.20	6.80	0.29
SO_3 %	1.90	0.38	2.00	0.15
Na_2O %	0.28	2.12	0.23	0.16
K_2O %	0.60	1.25	0.33	0.37
TiO_2 %	0.37	1.29	1.47	0.00
MnO %	0.10	0.00	0.34	0.17
Fe_2O_3 %	2.60	5.56	0.10	0.06
P_2O_3 %	0.20	0.00	0.00	0.05
C %	0.01	0.67	0.00	0.00
S %	0.00	0.00	0.00	0.00
Total %	99.26	98.31	98.87	99.35

Table 2 Physical Properties of Aggregates

	Coarse Aggregate	Fine Aggregate
Specific Gravity (SSD)	2.65	2.62
Size, mm	4.7-9.7	<4.7
Absorption, %	0.681	-

Table 3 Physical and Chemical Properties of Steel Bars.

Yield Point, N/mm^2	Tensile Strength N/mm^2	C %	Si %	Mn %	P %	S %
367	525	0.21	0.18	0.72	0.021	0.032

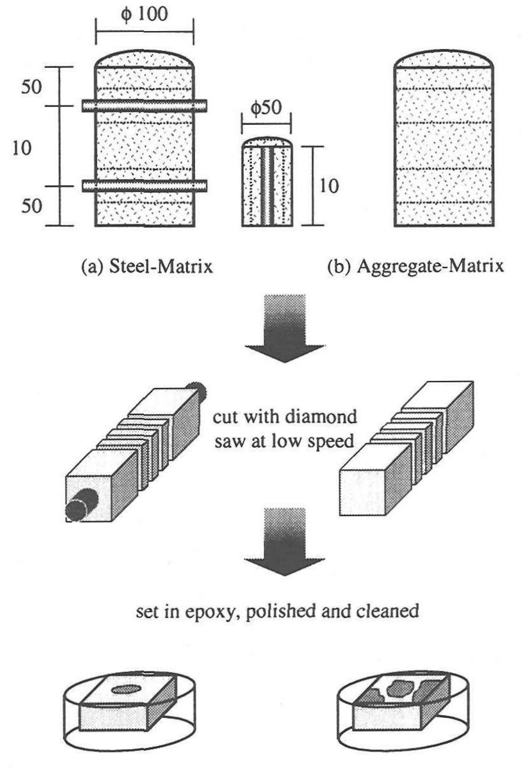

Fig. 2 *Specimen Configuration (unit: mm)*

4. EXPERIMENTAL PROCEDURE

(1) Materials

a) Cement

A research-grade ordinary portland cement provided by the Cement Association of Japan (CAJ) was used. **Table 1** shows the chemical composition as well as the physical properties of this OPC together with those of mineral admixtures used in this study.

b) Water

Tap water was used in all mixes.

c) Aggregates

Crushed sandstone coarse aggregate and ordinary river sand having the properties shown in **Table 2** were used. Aggregates were washed during sieving, subsequently dried to approximately saturated-surface-dry (SSD) condition, and stored in sealed plastic containers prior to their use to maintain the moisture content.

d) Mineral Admixtures

Fly ash (FA), blast furnace slag (BFS) and undensified silica fume (SF) were used as mineral admixtures. The properties of these admixtures are shown in **Table 1**.

e) Steel Bars

Round, plain, 6mm diameter steel bars (SR235) were used throughout the study. The physical and chemical properties are shown in **Table 3**. Rust and other dirt on the surface were removed by polishing with #240 SiC abrasive paper. The steel pieces were then wiped thoroughly with a clean cloth and stored in a desiccator until casting.

(2) Specimens

a) Specimens for Aggregate-Matrix ITZ Study

As shown in **Table 4**, seven mix proportions were used for the investigation. Cases 1-3 were all OPC pastes with varying W/C ratios. Common mineral admixture replacement ratios (FA: 30%, BFS: 50%, and SF: 10%) by volume were employed for cases 4-6 while case 7 corresponds to the paste part of a highly flowable concrete mix (OPC: 60%, BFS: 30%, and SF: 10%).

Mixing was done as follows: water and binder were mixed for 30s, stopped for 90s to remove paste adhering to the mixer wall, aggregates were added, then mixed again for 120s. ϕ100mm x 200mm specimens shown in **Fig. 2**(b) were cast. In all cases, placement was done in two lifts and each lift was vibrated for one minute on a vibration table.

Table 4 Mix Proportions of Aggregate-Paste Specimens

No.	Water-Binder Ratio	Unit content (kg/m^3)						Slump† or Flow
		Water	Cement	Coarse Agg.*	Mineral Admixture			
	W/B	W	C	G	FA	BFS	SF	(cm)
1	0.3	274	912	1154	-	-	-	9.2†
2	0.5	386	772	976	-	-	-	70.0
3	0.7	468	668	846	-	-	-	75.0
4	0.5	363	560	1012	167	-	-	52.5
5	0.5	376	392	992	-	361	-	39.5
6	0.5	379	702	987	-	-	56	40.0
7	0.5	373	472	997	-	217	57	31.5

*Size of Coarse Aggregates: 4.7-9.7mm.
Aggregate/Binder Ratio is 1.5 by volume for all cases.

Table 5 Mix Proportions of Steel Paste Specimens

No.	Water-Binder Ratio	Unit content (kg/m^3)					Flow	Bleeding Rate
		Water	Cement	Mineral Admixture				
	W/B	W	C	FA	BFS	SF	(cm)	(%)
1	0.3	485	1617	-	-	-	18.8	0
2	0.5	611	1222	-	-	-	>30.0	8.12
3	0.7	687	982	-	-	-	>30.0	19.89
4	0.5	587	905	271	-	-	28.5	9.58
5	0.5	601	626	-	576	-	22.3	2.19
6	0.5	604	1119	-	-	89	24.8	3.16
7	0.5	598	757	-	348	91	21.3	1.74

After casting, the specimens were cured for 24 hours in an enclosure of 90%+ relative humidity. After demolding, the specimens were kept in curing cabinets controlled at 20°C, 30°C and 60°C until the day of testing.

In designing the mix proportions, the water/binder and aggregate/binder ratios were fixed and thus, the slump or flow was not controlled.

b) Specimens for Steel-Matrix ITZ Study

The mix proportions are shown in the **Table 5**. These are similar to the ones listed in **Table 4** except for the exclusion of the aggregate.

Horizontal and vertical steel bar orientations were considered in this study. In the case of horizontal bars, holes slightly larger than ϕ6mm were drilled at the 50mm and 150mm marks from the bottom of the standard ϕ100mm x 200mm mold cans. Steel bars were then inserted and the joints sealed with epoxy to contain the water during casting. On the other hand, for the vertical case, steel bars were set in the middle of ϕ50mm x 100mm molds. (see **Fig. 2**(a)). Curing was same as that of the aggregate-paste specimens.

c) Specimens for Comparing Aggregate-Matrix and Steel-Matrix ITZs

The specimen configuration was the same as that for steel-paste investigation except for an additional "aggregate bar" (see **Fig. 3**(a)) placed such that its underside was at almost the same depth as the steel bar's underside. These "aggregate bars"

Table 6 Mix Proportions of Specimens Used in Comparing Steel- Paste and Aggregate-Paste ITZs.

No	W/B	Unit content (kg/m^3)						M†	Flow
		W	C	S	G	FA	SF	(%)	(cm)
1	0.3	274	912	-	1154	-	-	-	9.2‡
2	0.5	386	772	-	976	-	-	-	70.0
3	0.7	468	668	-	846	-	-	-	75.0
4	0.5	363	560	-	1012	167	-	-	52.5
5	0.5	379	702	-	987	-	56	-	40.0
6	0.5	379	702	-	987	-	56	1.5	44.5
7*	0.5	386	771	386	586	-	-	-	74.0
8*	0.5	379	702	390	592	-	56	-	53.5
9*	0.5	379	702	390	592	-	56	1.5	56.0

Notes: 1) Please refer to Tables 4 or 5 for definition of symbols.
2) Aggregate/Binder Ratio is 1.5 by volume for all cases.
*Sand/Aggregate Ratio is 0.4
†Chemical Admixture (Mighty 150), % of binder by weight
‡Slump

(a)
(b)
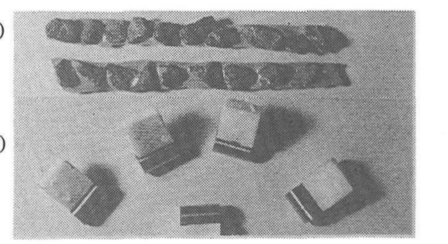

Fig. 3 a) aggregate bars and b) floating steels

were fabricated by setting aggregates in epoxy.

Also, aggregates were included in the mix together with "floating steels" (**Fig. 3**(b)). "Floating steels" were made from ϕ6mm x 10mm long polished steel bars attached to a 10mm x 10mm x 5mm styrofoam prisms. The size of the styrofoam was set such that the unit weight of the "floating steel" is approximately equal to that of the aggregate (2.65). The mix proportions used are shown in **Table 7**.

(3) Sample Preparation Procedures

a) Cutting

From the specimens shown in **Fig. 2**, bars containing the ITZ to be tested were cut using a diamond cutter. These bars were then cut crosswise by means of an ISOMET™ Low Speed Saw set at about 200 rpm. Water was used as a coolant during the cutting process. To remove dirt after cutting, the specimens were then cleaned using an ultrasonic cleaner. Since the succeeding procedures would take time, samples were stored in acetone to stop hydration.

In preparing the aggregate-matrix specimens for microhardness test, difficulty was encountered in making sure that the section really showed the lowermost portion of the aggregate.

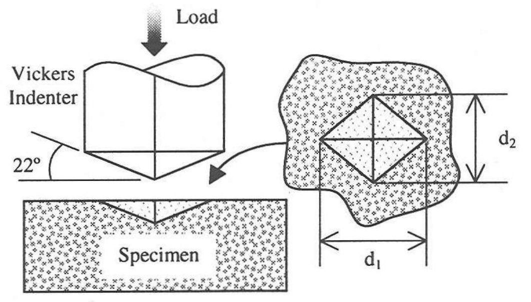

Fig. 4 The Vickers Microhardness Test

Fig. 5 Gap Measurement Using an Optical Microscope

Thus, for each aggregate under consideration, three sections were cut and from these, one was chosen, processed, and tested.

b) Setting in Epoxy

In order to avoid damage or specimen breakage during polishing, samples were set in an epoxy compound (Buehler's Epoxide Resin and Epoxide Hardener).

c) Polishing

After the epoxy hardened, the samples were then polished successively with SiC abrasive and finally with diamond paste (3μm diamond particles) in a METASERV® 2000 Grinder and Polisher.

Again, after polishing, the samples were cleaned in an ultrasonic cleaner and subsequently stored in a desiccator until the time of testing. It was deemed necessary to store the polished specimens for microhardness testing under the same humidity and temperature since the amount of moisture might affect the test results.

(4) Methods

a) The Vickers Microhardness Test

A Vickers indenter was used and the test was performed as shown in **Fig. 4**. The diagonals (d_1 and d_2) were measured and the average was taken. Using the average diagonal and knowing the angle of inclination of the indenter faces, the contact surface area was calculated. Then the hardness, which is defined as the ratio of the applied load to the contact surface area, was obtained.

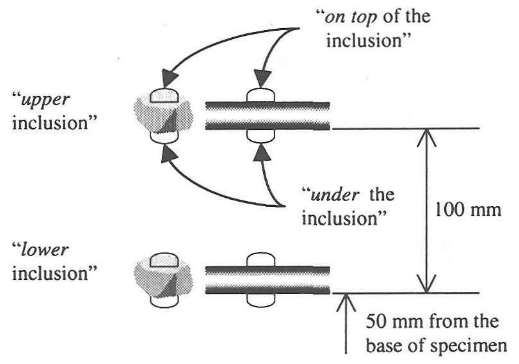

Fig. 6 Meaning of Terms Used in the Discussion

Testing was done using a load of 10 gram-force (the smallest possible for the machine used) with 10 seconds contact time.

It should be noted that for measurement points close to each other, overlapping of indentations might occur, which will not give the true hardness value. This was avoided by taking the measurements along a zigzag line. Care was taken to confirm the distance between the measurement point from the face of the inclusion and that the distance between adjacent indentations was at least twice the average diagonal. Two specimens for each case were tested and each point plotted in the graphs that will be shown later is the average of at least three values.

b) Scanning Electron Microscopy

Previously cut composite bars (~50 mm from the base of the specimens) which were stored in acetone were dried in an oven at 100°C for 1 day and cooled down to room temperature were fractured with a chisel and hammer. Caution was taken in order to avoid contact between the chisel and the location to be observed. Fracture surfaces were subsequently coated with carbon for SEM examination.

c) Visual Observation and Other Optical Methods

Macroscopic features such as the presence of large pores were observed and photos were taken for documentation. These photos were used as aids in describing the appearance of paste surfaces in contact with the steel or aggregate.

In some specimens, gaps were observed under the horizontal steel bars and aggregates. The widths of these gaps were measured with an optical microscope and the scale 100μm per division was used. This is illustrated in **Fig. 5** for the steel-paste and aggregate-paste cases.

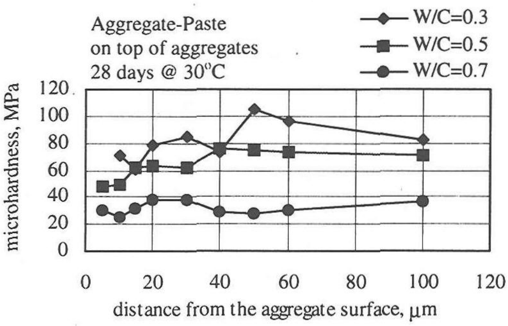

Fig. 7 Microhardness of Aggregate-Paste Transition Region

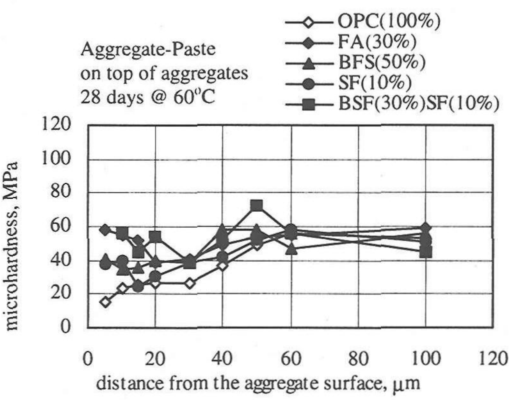

Fig. 8 Effect of Mineral Admixtures on the Microhardness of the Transition Region

(5) Notes on Observation Procedure

Fig. 6 defines the terms used in the discussions that follow. Take note of the difference between the use of the terms "under" and "lower". The former refers to the region below an inclusion while the latter refers to the location of the inclusion, which is located 50mm from the base of the specimen.

In comparing the vertical and horizontal steel bars with respect to microhardness, the ϕ50mm x 100mm specimens with centrally located vertical steel bars were cut at the 50mm mark from the base of the specimen. The transition regions on top and under the lower horizontal bars were used for comparison.

5. THE AGGREGATE-PASTE ITZ

(1) Introduction

Experimental results and discussions related to the aggregate-paste ITZs are presented and discussed with respect to a) transition region properties, which include thickness and microhardness and b) gaps formed under the aggregates. It is the objective of this section to describe the ITZs and some of its characteristics.

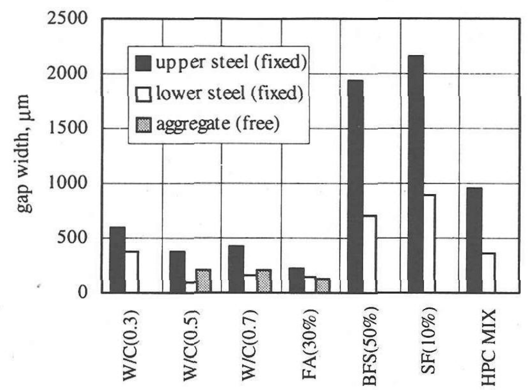

Fig. 9 Gaps Under the Inclusions (paste case)

(2) Discussion of Factors

a) W/C

The effect of W/C is first explained using the microhardness test results as shown in **Fig. 7**. Measurements were taken at the paste region *on top of the aggregates* that were located at 150mm from the base of the specimens. The general trend is that the higher the W/C is, the lower are the microhardness values. It is also observed that the microhardness generally become lower as the aggregate surface is approached.

The point at which the hardness values started to decrease as the aggregate is approached is designated as the upper limit of the transition region thickness. For the cases in consideration, these points are not distinct. Basing however from the general trend, for the case of W/C = 0.3 this point can be taken at around 50μm, 40μm for W/C = 0.5 and 20μm or less for W/C = 0.7, which shows that as the W/C increases, the thickness decreases. This suggests that increasing the W/C makes both the transition region and the bulk matrix softer and the microhardness distribution near the aggregate becomes more uniform.

b) Mineral Admixtures

It can be observed from **Fig. 8** that the microhardness of the cases with mineral admixtures lie above that of the control (100% OPC, W/C=0.5) especially near the aggregate surface. However, at the region far from the aggregate surface the values are almost the same. Thus, in terms of microhardness, addition of mineral admixtures makes the transition region (< 50μm) harder but does not affect the bulk matrix significantly.

Another effect of mineral admixtures is in the size of gaps formed under the aggregates. Compared to the control (100% OPC, W/C=0.5), it

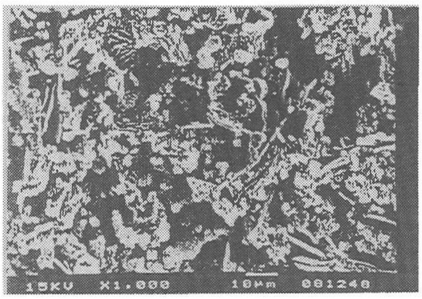

Fig. 10 SEM photo (100% OPC, W/C=0.5)

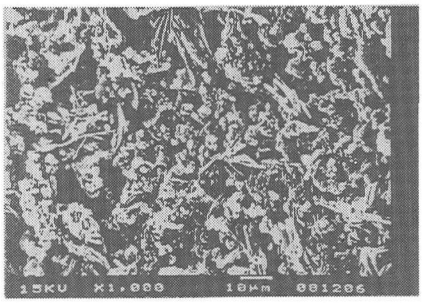

Fig. 11 SEM photo (90% OPC, 10% SF W/B=0.5)

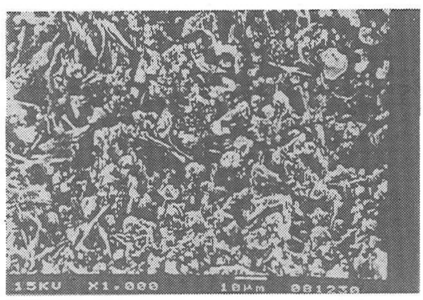

Fig. 12 SEM photo (60% OPC, 30% BFS, 10% SF, W/B=0.5)

can be seen from **Fig. 9** that addition of admixtures reduced the gap sizes, as in the case of fly ash, or totally eliminated the gaps. Probable reasons for this phenomenon are discussed in Chapter 7.

As for the SEM observation, **Figs. 10-12** show the paste side of fracture surfaces. These surfaces were formerly in contact with the aggregates and since these were the surfaces where fracture occurred, then these can be thought of as the weakest surfaces.

Taking **Fig. 10** as the reference, the effect of addition of admixture improved the transition region by making it denser. The pores (black spots) and hydration products are smaller in **Figs. 11&12**.

c) Location

Fig. 13 shows the comparison of transition region microhardness measured *on top* and *under* the aggregates. It was observed that out of the 7 aggregate-paste systems considered, gaps formed under the aggregate for 3 cases (see **Fig. 9**):

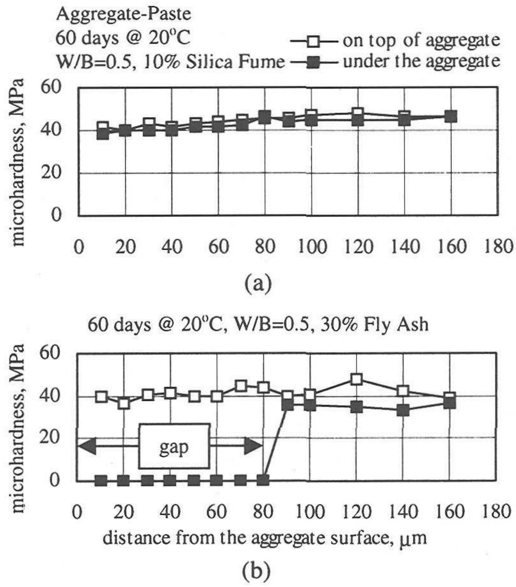

Fig. 13 Comparison of Microhardness With Respect to Location: (a) zero gap case (b) with gap case

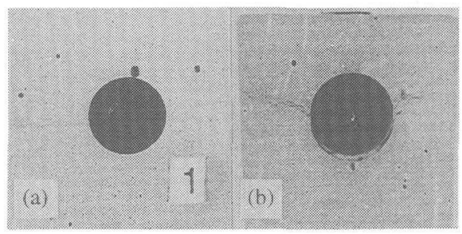

Fig. 14 Section Across a (a)Vertical Bar and (b) Horizontal Bar (100% OPC, W/C = 0.5, 28 days @ 20°C)

a) 100% OPC, W/C = 0.5; b) 100% OPC, W/C = 0.7; and c) 30% Fly Ash, W/B = 0.5. **Fig. 13**(a) is a representative of the cases with no gaps. For these cases, there was no significant difference between the transition region microhardness on top and under the aggregates. For those with gaps however (**Fig. 13**(b)), the appearance of the gaps under the aggregate led to lower microhardness at the lower transition region. Development of gaps under the aggregates is a very important subject and is discussed further later in this paper.

6. THE STEEL-PASTE ITZ

(1) Steel Orientation

Steel orientation is defined with respect to casting direction. Horizontal bars and vertical bars refer to steel bars perpendicular and parallel to the casting direction respectively. The main difference between the two lies in the nature of the paste surfaces at or near the steel surface.

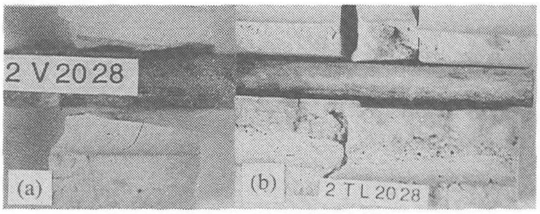

Fig. 15 Surface in Contact with (a) Vertical Bar and (b) Horizontal Bar; (100% OPC, W/C = 0.5, 28 days @ 20°C)

Table 7 Gap Sizes Under Upper and Lower Bars (paste case)

W/C	Upper Bar μm	Lower Bar μm	Upper Bar Gap/ Lower Bar Gap
0.3	587	373	1.6
0.5	381	114	3.3
0.7	422	158	2.7

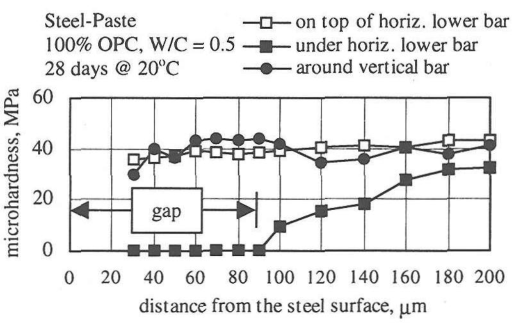

Fig. 16 Comparison Between Transition Region Microhardness of Horizontal and Vertical Bars

a) Physical Description

Fig. 14 shows representative cross-sections of specimens with horizontal and vertical steel bars. The paste surrounding the vertical steel bar is continuously in contact with the steel bar. On the other hand, only the upper paste portion was in contact with the horizontal steel bar. A large gap under the horizontal steel bar is clearly visible.

After breaking the specimens lengthwise, the paste surfaces were observed and representative surfaces are shown in **Fig. 15**. The paste surface in contact with the vertical steel bar is consistently smooth. However, large pores and rough surfaces (lower right of **Fig. 15**(b)) characterized the paste surface under the horizontal bar.

Since the soundness of the matrix covering the steel is important in corrosion protection, the underside of the horizontal steel bars in reinforced concrete may be critical areas.

b) Mechanical Difference

Microhardness measurements taken at the vicinity of the steel bars located at 50mm from the base of the specimens are shown in **Fig. 16**. Gaps were present under the horizontal bars and micro-

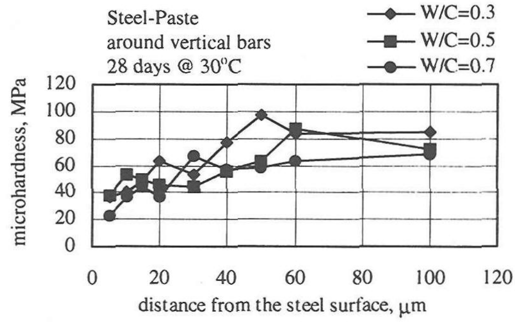

Fig. 17 Microhardness of the Steel-Paste Transition Region

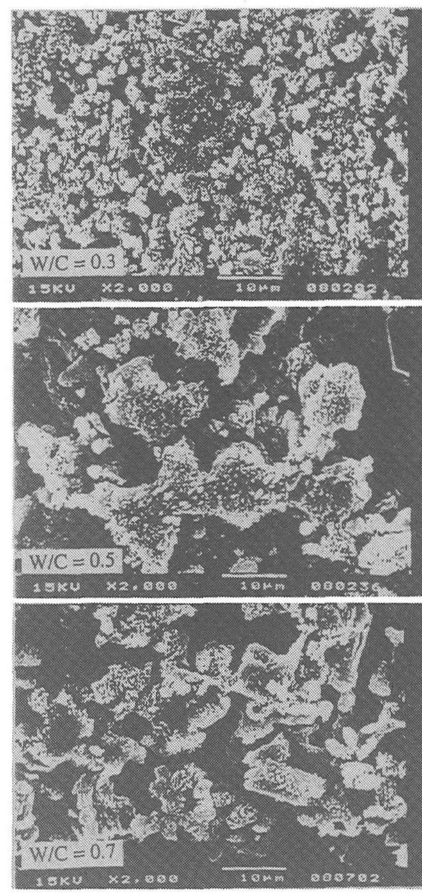

Fig. 18 SEM Photos of the Paste in Contact with the Steel (28 days @ 20°C)

hardness of the gaps were designated as zero. It is observed that that the microhardness of the transition region around the vertical bars are comparable to that on top of the horizontal bars. However, the presence of gaps led to lower microhardness values under the horizontal bars.

(2) Steel Position

Comparing horizontal bars placed at different depths (upper bars were 10 cm higher than

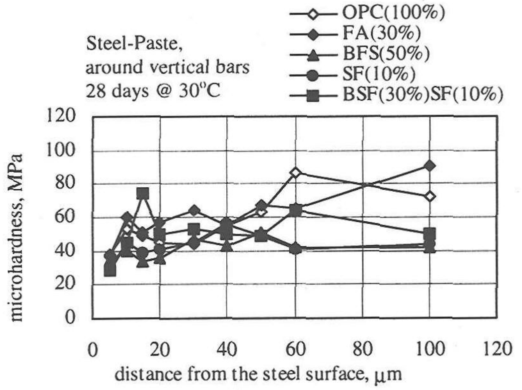

Fig. 19 Microhardness of the Vertical Steel-Paste Transition Region for Systems with Mineral Admixtures

Table 8 Gap Sizes Under Upper and Lower Bars (concrete case)

W/C	Upper Bar Gap, μm	Lower Bar Gap, μm
0.4	400	0
0.5	200	0
0.7	200	0

lower bars), the gaps formed under bottom bars were narrower. **Table 7** shows the thickness of gaps under the horizontal bars for three W/C ratios. Discussion about these gaps will be made in Chapter 7.

From these results it can be said that as the distance of the horizontal bar from the base of the specimen becomes larger, the ITZ quality becomes worse and this may be an important point to consider in deciding the maximum height of lift during concrete casting.

(3) W/C

As shown in **Table 7**, W/C is not directly related to gap size. This observation also holds true for concrete as will be discussed later. This may be attributed to a combined effect of factors such as bleeding and autogeneous shrinkage, which is out of the scope of the present investigation.

In the case of transition region microhardness, specimens with low W/C were harder as shown in **Fig. 17** (Note: From hereon, microhardness values are those of the transition regions near vertical steel bars unless otherwise specified.).

Fig. 18 shows representative pictures of the paste surfaces that were in contact with vertical steel bars. While it is true that the hydration products tend to be smaller and the morphology more compact as W/C decreases, it is observed that for the case of W/C = 0.5 and 0.7, the structures are comparable.

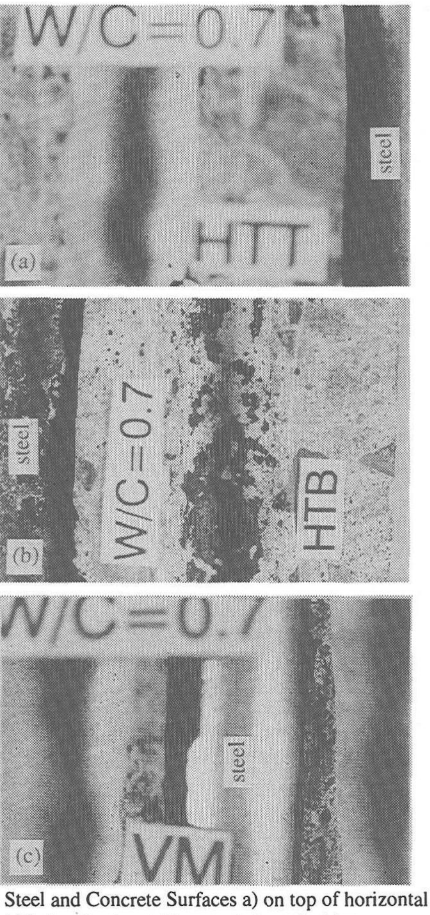

Fig. 20 Steel and Concrete Surfaces a) on top of horizontal bar, b) below horizontal bar, and c) vertical bar

(4) Mineral Admixtures

As for the microhardness results, **Fig. 19** shows that except for the case of fly ash, addition of admixtures led to a more uniform microhardness distribution. The values at the right of the 60μm mark which can be taken as that of the bulk paste does not vary much with that at the left (transition region) as opposed to the case of OPC only and the case with fly ash. It can be thought that this is due to the physical properties of the admixture. Fly ash, having fineness of same magnitude as OPC did not lead to transition zone modification as compared to other admixtures with larger fineness.

With regard to gaps under the horizontal steel bars, it can be seen from **Fig. 9** that except for the case of fly ash, addition of mineral admixtures resulted in large gaps. This result is in contrast with that of the aggregates wherein the addition of mineral admixtures reduced or eliminated the gaps. More detailed discussions on the comparison between the aggregate-matrix and steel-matrix ITZs will be done in the next chapter.

(5) Extension of Steel-Paste Study to Reinforced Concrete

The same trend was observed for both paste and concrete specimens in relation to steel bar orientation (vertical vs. horizontal), steel bar location (upper vs. lower), and W/C. Some of these are 1) paste/concrete surfaces in contact with vertical bars and on top of upper bars were smooth while rough surfaces characterized by visible voids were observed at paste/concrete surfaces under horizontal bars, and 2) gaps formed under upper bars were wider than those which were under lower bars, and 3) W/C=0.3 case had the widest gaps (**Tables 7** and **8**).

An interesting observation can be said with regard to corrosion. It is common knowledge that the rate of corrosion of reinforcement depends on migration of harmful substances at the interface. Compact ITZ means more protection from corrosion. **Fig. 20** shows the steel bars and concrete surfaces taken from specimens with 10kg/m^3 NaCl added to the concrete mix and cured at room temperature at around 90% RH for 6 months. The vertical steel bar does not show visual signs of corrosion compared to the horizontal steel bars. In the case of horizontal steel bars however, the lower surfaces are corroded while the top parts are uncorroded.

With respect to steel bar location, the bottom portions of upper bars corroded more than that of the lower bars.

In summary, steel bar regions with sound ITZs showed no or little corrosion while those with gaps were all corroded. From this it can be said that in protecting the steel bar from corrosion, not only the transition region should be strengthened or densified but also gaps should be eliminated or at least minimized.

7. COMPARATIVE STUDY BETWEEN THE AGGREGATE-MATRIX AND STEEL-MATRIX ITZ

(1) Introduction

In the literature, studies on ITZs were concentrated on particular ITZs only. In this paper, an attempt to compare the two ITZs is made which led to some interesting results. The comparison was made with respect to both the gaps and the transition regions.

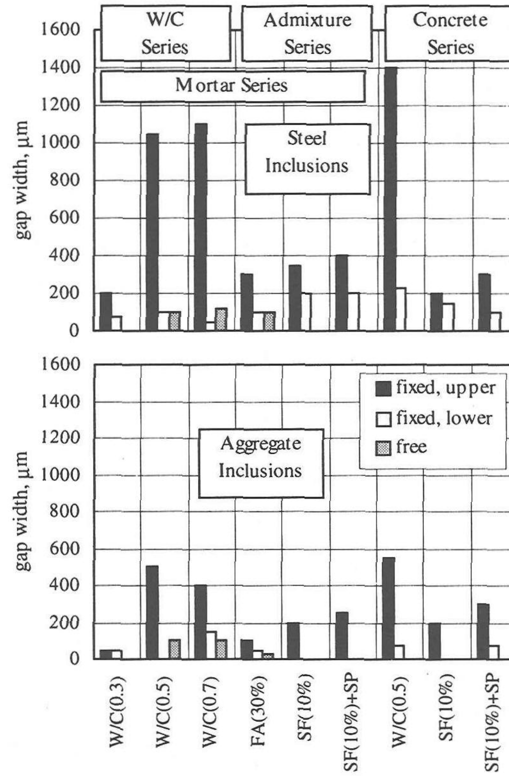

Fig. 21 Gaps Under the Inclusions

(2) Discussion on Gaps

a) Formation of Gaps

It has been observed that large gaps were formed under the horizontal steel bars (**Tables 7** & **8**). The presence of these gaps can be very critical not only from the point of view of strength but also of durability. However, for the case of aggregates, gaps were found only in three mixes: that of W/C=0.5 and 0.7 using OPC and W/B=0.5 utilizing fly ash with 30% replacement ratio. From **Fig. 21**, the widest gap in the aggregate case was an order of magnitude lower than that of horizontal steel bar case. This phenomenon was thought to be caused by the difference in relative movement of *inclusions* (hereafter used to refer to either or both steel bar and aggregate) with respect to the paste matrix. In order to validate this, an experiment with fixed and free inclusions as described in earlier was conducted. It should be noted however that in the case of fixed/free aggregate particles and free steel inclusion, due to the difficulty in specimen preparation, the observed section may not reveal the true gap width. However, by carefully selecting from a number of sections, the results shown in **Fig. 21** can be thought not to differ much from the true gap widths.

b) Fixed vs. Free Inclusions

As can be noted in **Fig. 21**, in almost all cases, larger gaps formed under the fixed steel bars compared to free ones. This was also confirmed for the aggregate case.

A possible explanation is that fixing an inclusion especially against the formwork may lead to more vibration of the matrix around it. And thus, fixing an inclusion during casting may lead to the formation of gaps under it. This observation is consistent with a previous study[6] where it was noted that vibration can lead to higher local water content and inefficient packing around the inclusion.

c) Gaps and Inclusion Surface Conditions

It is observed that in all cases considered, the gaps formed under the aggregates are equal to or smaller than the ones formed under the corresponding steels regardless of whether they are fixed or free (**Fig. 21**). It seems likely that the cause is the difference in surface properties of the aggregates and steels. Rough surfaces provide more nucleation sites as compared to smoother surfaces and also, the aggregate may absorb some water, which will reduce the local W/C near it.

d) Effect of Inclusion Content on Gap Formation

This is basically a comparison between the gaps formed in pastes, mortars, and concretes. It is important to note that the volume of aggregate (fine+coarse) was the same for mortar and concrete mixes. Only coarse aggregates were present in mortar specimens which means that the concrete mixes have more fine particles compared to mortars. Addition of aggregates in order to produce mortars or concretes led to smaller gaps. For example, a difference in gap widths of 84% was observed for silica fume paste and mortar specimens (refer to **Figs. 9** and **21**). On the other hand, for mortars and concretes, the difference was around 43%. A point of contrast however existed for the OPC only case with W/C=0.5, there was actually an increase in the gap size.

From the above observations, it can be said that the aggregate content and grading may reduce the gap size but more tests are needed to support this idea.

e) Effect of Chemical Admixture

With regard to gap formation, the effect of superplasticizer(SP) is also shown in **Fig. 21** for silica fume replaced systems. For the case of free inclusions, there were no gaps observed. On the other hand, for fixed inclusions and for both mortar and concrete cases, almost all the systems with superplasticizer showed a little increase in gaps widths. However, the increase of at most 100μm is not so significant and can be easily attributed to other factors. A deeper investigation will be done regarding this matter.

(3) Discussion With Respect to the Transition Regions

The discussions above focused on the gaps formed below the inclusions. Here, the difference between the matrices affected by the presence of the inclusion is discussed. **Figs. 7** and **17** shows the microhardness results for the OPC series at 28 days for steel-paste and aggregate-paste ITZs respectively.

It is observed that for the case of steel bar-paste ITZ, there is a steeper decrease in microhardness as the interface is approached in contrast with that of the aggregates wherein there is a more uniform distribution. From this it can be concluded that aggregate-paste transition regions are better than that of the steels since the transition region microhardness in the former is not so different from that of the bulk matrix. In connection with the discussions of gap formation, this result can also be due to the fixed nature of the steel bars, the fact that the aggregates were present during mixing and free to move during casting, and the difference in the surface condition of the inclusions.

8. CONCLUSIONS

In this paper, it was shown that there is a difference between the aggregate-matrix and steel bar-matrix ITZs specifically with regard to the addition of mineral admixtures and gap formation. Incorporation of mineral admixtures reduced or inhibited gap formation in aggregate-matrix systems while addition of mineral admixtures resulted in large gaps below horizontal bars, except for the case of fly ash addition.

Also, the ITZs around the aggregates are shown to be better than that of the steel bars due to narrower gaps/absence of gaps and more uniform microhardness distribution in the former. Fixity of the inclusion during casting was shown to be a major factor contributing to gap formation.

ACKNOWLEDGMENT: The authors wish to express their most sincere gratitude to Prof. Shigeyoshi Nagataki, Prof. Kazuhiko Kawashima, Prof. Osamu Kusakabe, and Dr. Kazuo Tateishi for their helpful discussions. Heartfelt thanks is also extended to all members of the Concrete Laboratory for their help in the experiments.

The support given by the Ministry of Education for making this study possible is also appreciated.

REFERENCES

1) Farran, J.: *Introduction: The transition zone - discovery and development*, in Interfacial Transition Zone in Concrete, Maso, J. C., ed., E & FN Spon, London, 1996.
2) Monteiro, P. J. M. and Mehta, P. K.: *Ettringite Formation on the Aggregate-Cement Paste Interface*, CCR, Vol. 15, pp. 378-90, 1985.
3) Mehta, P. K.: Concrete: Materials, Structure and Properties, Prentice-Hall Inc., 1986.
4) Breton, D., Carles-Guibergues, A., Ballivy, G. and Grandet, J.: *Contribution to the Formation Mechanism of the Transition Zone Between Rock-Cement Paste*, CCR, Vol. 23, pp. 335-46, 1993.
5) Scrivener, K. L. and Pratt P. L.: *Characterization of Interfacial Microstructure*, in Interfacial Transition Zone in Concrete, Maso, J. C., ed., RILEM Technical Committee 108-ICC Report, E&FN Spon (Chapman & Hall), 1996.
6) Pinchin, D. J. and Tabor, D.: *Interfacial Phenomena in Steel Fibre Reinforced Cement I: Structure and Strength of Interfacial Region*, CCR, Vol. 8, pp. 15-24, 1978.
7) Barnes, B. D.: *The Contact Zone Between Portland Cement Paste and Glass "Aggregate" Surfaces*, CCR, Vol. 8, pp. 233-44, 1978.
8) Barnes, B. D., Diamond, S. and Dolch, W. L.: *Micromorphology of the Interfacial Zone Around Aggregates in Portland Cement Mortar*, J. Am. Ceram. Soc., Vol. 62, No. 1-2, pp. 21-4, 1979.
9) Scrivener, K. L. and Pratt, P. L.: Proc., 8th ICCC, Rio, Vol. 111, pp. 466-71, 1986.
10) Scrivener, K. L., Crumbie, A. K. and Pratt, P. L.: *A Study of the Interfacial Region Between Cement Paste and Aggregate in Concrete*, in Bonding in Cementitious Composites, Mindess, S. and Shah, S. P., eds., Materials Research Society Symposium Proceedings, Vol. 114, 1988.
11) Struble, L.: *Microstructure and Fracture at the Cement Paste-Aggregate Interface*, in Bonding in Cementitious Composites, Mindess, S. and Shah, S. P., eds., Materials Research Society Symposium Proceedings, Vol. 114, 1988.
12) Scrivener, K. L. and Gartner, E. M.: *Microstructural Gradients in Cement Paste Around Aggregate Particles*, in Bonding in Cementitious Composites, Mindess, S. and Shah, S. P., eds., Materials Research Society Symposium Proceedings, Vol. 114, 1988.
13) Bentur, A. and Odler, I.: *Development and Nature of Interfacial Microstructure*, in Interfacial Transition Zone in Concrete, Maso, J. C., ed., RILEM Technical Committee 108-ICC Report, E&FN Spon (Chapman & Hall), 1996.
14) Odler, I. and Zurz, A.: *Structure and Bond Strength of Cement-Aggregate Interfaces*, in Bonding in Cementitious Composites, Mindess, S. and Shah, S. P., eds., Materials Research Society Symposium Proceedings, Vol. 114, 1988.
15) Alexander, M. G.: *Two Experimental Techniques for Studying the Effects of the Interfacial Zone Between Cement Paste and Rock*, CCR, Vol. 23, pp. 567-75, 1993.
16) Mindess, S.: *Tests to Determine the Mechanical Properties of the Interfacial Zone*, in Interfacial Transition Zone in Concrete, Maso, J. C., ed., RILEM Technical Committee 108-ICC Report, E&FN Spon (Chapman & Hall), 1996.
17) Ollivier, J. P. and Massat, M.: *The Effect of the Transition Zone on Transfer Properties of Concrete, in Interfacial Transition Zone in Concrete*, Maso, J. C., ed., RILEM Technical Committee 108-ICC Report, E&FN Spon (Chapman & Hall), 1996.
18) Massaza, F.: *Action of Environmental Conditions, in Interfacial Transition Zone in Concrete*, Maso, J. C., ed., RILEM Technical Committee 108-ICC Report, E&FN Spon (Chapman & Hall), 1996.
19) Mindess, S.: *Interfaces in Concrete*, in Materials Science of Concrete, Vol. 1, Skalny J. P., ed., Materials Research Society, 1989.
20) Monteiro, P. J. M., Gjorv, O. E. and Mehta, P. K.: *Microstructure of the Steel-Cement Paste Interface in the Presence of Chloride*, CCR, Vol. 15, pp. 781-4, 1985.
21) Wei, S., Mandell, J. A. and Said, S.: *Study of the Interface Strength in Steel Fiber-Reinforced Cement-Based Composites.*, ACI Materials Journal, July-August 1986.
22) Page, C. L. and Vennesland, O.: *Pore Solution Composition and Chloride Binding Capacity of Silica Fume-Cement Pastes*, SINTEF, STF A82025, The Norweigian Institute of Technology, NTH, Trodheim, 1982 as cited in ref. 17.
23) Page, C. L.: *Mechanism of Corrosion Protection in Reinforced Concrete Marine Structures*, Nature, Vol. 258, Dec. 11, 1975.

(Received November 6, 1996)

鉄筋コンクリート中の界面(遷移帯)に関する実験的研究

大即　信明・久田　真・ Nathaniel B. DIOLA ・ Tarek UDDIN Md.

本研究は，鉄筋コンクリート中における粗骨材-マトリクスと鉄筋-マトリクス間に形成される界面(遷移帯及び空隙)の特性と相違，これらに及ぼす各種要因の影響の程度を把握することを目的とした．

界面に影響を及ぼす要因として，混和材の使用，配合条件，打設時の鉄筋の方向等を取り上げた．

本論文を通じて，鉄筋コンクリート中における界面(遷移帯)の形成状況，界面の分布等の基本的な特性を把握することができ，骨材-マトリクス間および鉄筋-マトリクス間に形成される界面を比較し，骨材および水平鉄筋の下部に形成される界面空隙の形成状況が大きく相違していることを明かにした．